Volume 10 | Number 12 | December 2014 | Pages 3033–3324

Molecular BioSystems

Interfacing chemical biology with the -omic sciences and systems biology

www.molecularbiosystems.org

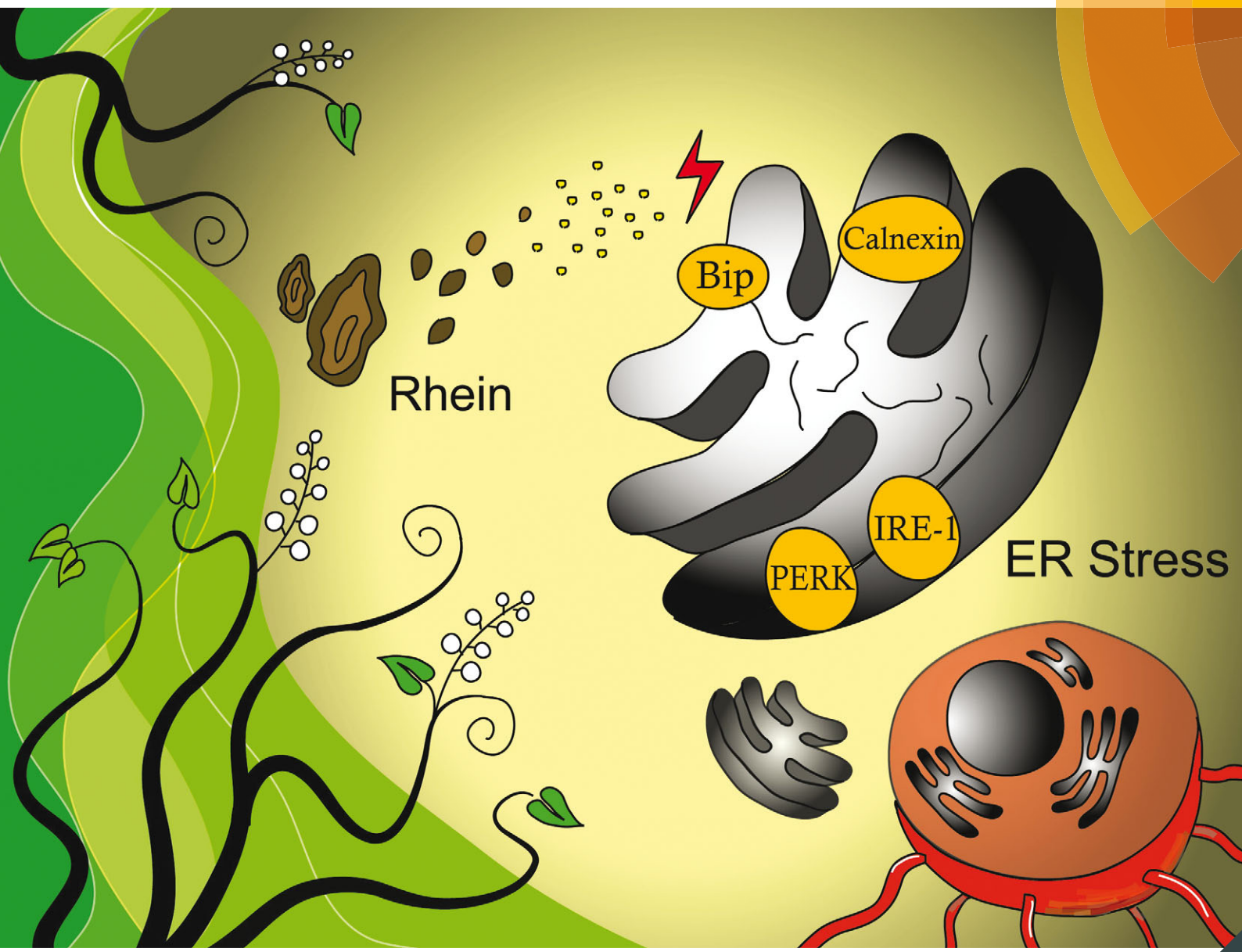

ISSN 1742-206X

ROYAL SOCIETY OF CHEMISTRY

PAPER

Hong-Lin Chan *et al.*

Proteomic analysis of rhein-induced cyt: ER stress mediates cell death in breast cancer cells

Indexed in Medline!

Molecular BioSystems

PAPER

View Article Online
View Journal | View Issue

Cite this: *Mol. BioSyst.*, 2014, **10**, 3086

Proteomic analysis of rhein-induced cyt: ER stress mediates cell death in breast cancer cells†

Hui-Ju Huang,‡[a] Chi-Chen Lin,‡[bcde] Hsiu-Chuan Chou,[f] Yi-Wen Chen,[a] Szu-Ting Lin,[a] Yi-Chieh Lin,[a] Dai-Ying Lin,[a] Kevin W. Lyu[gh] and Hong-Lin Chan*[a]

Received 31st July 2014,
Accepted 17th September 2014

DOI: 10.1039/c4mb00451e

www.rsc.org/molecularbiosystems

Rhein is a natural product purified from herbal plants such as *Rheum palmatum*, which has been shown to have anti-angiogenesis and anti-tumor metastasis properties. However, the biological effects of rhein on the behavior of breast cancers are not completely elucidated. To evaluate whether rhein might be useful in the treatment of breast cancer and its cytotoxic mechanism, we analyzed the impact of rhein treatment on differential protein expression as well as redox regulation in a non-invasive breast cancer cell line, MCF-7, and an invasive breast cancer cell line, MDA-MB-231, using lysine- and cysteine-labeling two-dimensional difference gel electrophoresis (2D-DIGE) combined with MALDI-TOF/TOF mass spectrometry. This proteomic study revealed that 73 proteins were significantly changed in protein expression; while 9 proteins were significantly altered in thiol reactivity in both MCF-7 and MDA-MB-231 cells. The results also demonstrated that rhein-induced cytotoxicity in breast cancer cells mostly involves dysregulation of cytoskeleton regulation, protein folding, the glycolysis pathway and transcription control. A further study also indicated that rhein promotes misfolding of cellular proteins as well as unbalancing of the cellular redox status leading to ER-stress. Our work shows that the current proteomic strategy offers a high-through-put platform to study the molecular mechanisms of rhein-induced cytotoxicity in breast cancer cells. The identified differentially expressed proteins might be further evaluated as potential targets in breast cancer therapy.

1. Introduction

Rhein is a natural product purified from herbal plants such as *Rheum palmatum*.[1] It has long been used to reduce metabolic disorders,[2] obesity,[3] angiogenic effects[4] and exhibits anti-bacterial activity.[5] Rhein has also been reported to show anti-tumor metastasis in human tongue cancer *via* the inhibition of gene expression of matrix metalloproteinase-9.[6] It has also been demonstrated that rhein inhibits invasion of human nasopharyngeal carcinoma cells by down-regulation of the vascular endothelial growth factor.[7] Recently, the generation of reactive oxygen species (ROS) has been reported to be an important factor in rhein-induced apoptosis of cancer cells.[8] However, the detailed mechanisms of rhein-induced cytotoxicity remain poorly understood.

Proteomics is a powerful strategy to examine protein expression alterations in response to various treatments or physiological conditions. 2-DE has long been recognized as an important technique in the proteomic field for large-scale protein profiling within biological samples as well as plays a complementary role to LC-MS-based proteomic analysis.[9] Nevertheless, reliable quantitative comparison across gels remains the main challenge in 2-DE analysis. A significant progress in 2-DE-based protein quantification and detection was accomplished by the introduction of 2D-DIGE, where numerous protein samples can be co-detected on the same 2-DE gel using differential fluorescent labeling (Cy2, Cy3 and Cy5). This advancement improves gel-to-gel variation and allows comparison of the relative amount of resolved proteins across different gels by using a fluorescently-labeled internal standard. In addition, the 2D-DIGE proteomic analysis has the benefits of a broader linear dynamic range of detection, greater

[a] *Institute of Bioinformatics and Structural Biology & Department of Medical Science, National Tsing Hua University, Hsinchu, Taiwan. E-mail: hlchan@life.nthu.edu.tw; Fax: +886-35-715934; Tel: +886-35-742476*
[b] *Institute of Biomedical Science, National Chung-Hsing University, Taichung, Taiwan*
[c] *Institute of Biomedical Science, and Rong Hsing Research Center for Translational Medicine, National Chung Hsing University, Taiwan*
[d] *Department of Medical Research and Education, Taichung Veterans General Hospital, Taichung, Taiwan*
[e] *Division of Chest Medicine, Department of Internal Medicine, Changhua Christian Hospital, Changhua, Taiwan*
[f] *Department of Applied Science, National Hsinchu University of Education, Hsinchu, Taiwan*
[g] *Lutheran Medical Center, Brooklyn, NY, USA*
[h] *Global Scholars Program, St. George's University/Northumbria University, Newcastle upon Tyne, UK*

† Electronic supplementary information (ESI) available. See DOI: 10.1039/c4mb00451e

‡ These authors contributed equally.

reproducibility and higher sensitivity than traditional 2-DE.[9] This innovative proteomic analysis relies on the pre-labeling of protein samples on the amino group of lysine residues with fluorescent dyes (Cy2, Cy3 and Cy5) before electrophoresis. Each of the three dyes has a distinct fluorescent wavelength, allowing comparison of experimental protein samples and an internal standard to be concurrently separated in the same gel. The internal standard, which is a pool of an equal amount of all protein samples, helps to provide precise spot matching and normalization as well as increases statistical confidence in relative quantification across different gels.[10–14] Recently, a cysteine labeling version of 2D-DIGE was developed, by using ICy dyes (iodoacetyl cyanine dyes) which react with the free thiol group of cysteines through alkylation. A pair of ICy dyes (ICy3 and ICy5) have been used to examine redox-dependent protein thiol modifications in a model cell system exposed to hydrogen peroxide and in plasma fractions exposed to UVC[15] as well as used in the analysis of redox-regulation of cancer cells.[16]

The main purpose of the current study was to use a proteomic analysis combining lysine and cysteine 2D-DIGE and mass spectrometry to investigate the inhibitory effects of rhein on breast cancer cells (MCF-7 and MDA-MB-231). MCF-7 and MDA-MB-231 cells, originally derived from pleural effusion of patients with low- and high-invasive breast ductal carcinoma, were used as model breast cancer systems to clarify the molecular effects of rhein including the monitoring of rhein-induced protein expression and redox modification of intracellular proteins.

2. Materials and methods

2.1 Chemicals and reagents

Generic chemicals including rhein were purchased from Sigma-Aldrich (St. Louis, USA), while reagents for 2D-DIGE were purchased from GE Healthcare (Uppsala, Sweden). The synthesis of the ICy3 and ICy5 dyes has been previously reported by our group.[15] All primary antibodies were purchased from Genetex (Hsinchu, Taiwan) and anti-mouse, and anti-rabbit secondary antibodies were purchased from GE Healthcare (Uppsala, Sweden). All the chemicals and biochemicals used in this study were of analytical grade.

2.2 Cell lines and cell cultures

The breast epithelial cell line MCF-10A was a gift from Dr Wun-Shaing Wayne Chang, National Health Research Institute, Taiwan. The breast cancer cell lines MCF-7 and MDA-MB-231 were purchased from American Type Culture Collection (ATCC), Manassas, VA. MCF-10A was maintained in Dulbecco's Modified Eagle's medium and F-12 medium (DMEM/F-12) supplemented with 5% horse serum, L-glutamine (2 mM), streptomycin (100 μg mL^{-1}), penicillin (100 IU mL^{-1}), the epidermal growth factor (20 ng mL^{-1}) (all from Gibco-Invitrogen Corp., UK), insulin (10 μg mL^{-1}) (Sigma) and hydrocortisone (0.5 μg mL^{-1}) (Sigma). MCF-7 and MDA-MB-231 were maintained in Dulbecco's Modified Eagle's medium (DMEM) supplemented with 10% (v/v) fetal calf serum (FCS), L-glutamine (2 mM), streptomycin (100 μg mL^{-1}), and penicillin (100 IU mL^{-1}) (all from Gibco-Invitrogen Corp., UK). All cells were incubated at 37 °C and 5% CO_2.

2.3 MTT cell viability assay

The detailed MTT procedure has been described in our previous publication.[16] MCF-10A cells, MCF-7 cells and MDA-MB-231 cells (5000 cells per well) growing exponentially were seeded into 96-well plates. The culture cells were incubated for 24 h before treatment with indicative concentrations (a dose range 0–100 μg mL^{-1}) of rhein for 24 h and untreated as control. After removal of the medium, 100 μL of MTT working solution (1 mg mL^{-1}) (Sigma) was added into each well, followed by further incubation at 37 °C in 5% CO_2 for 4 h. The supernatant was carefully removed followed by addition of 100 μL of DMSO to each well and shaken for 15 min. The absorbance of samples was measured at a wavelength of 540 nm in a multi-well plate reader. Values were normalized against the untreated samples and were averaged from 8 independent measurements.

2.4 Immunofluorescence

The detailed immunofluorescence procedure has been described in our previous publication.[17] For immunofluorescence staining, cells were fixed with 4% paraformaldehyde for 25 min and the attached cells washed twice with PBS, and then permeabilized with 0.1% Triton X-100 for 10 min, blocked with 5% bovine serum albumin in PBS for 1 h, followed by incubation with primary antibodies at 4 °C for 24 h. After three PBS washes, samples were incubated with appropriate fluorescently labeled secondary antibodies diluted (1 : 100) in 2.5% BSA/PBS. Coverslips were then washed three times with PBS and at least twice with ddH_2O before being mounted with 4 μL antifade mounting reagent (Invitrogen) and dried in the dark at 4 °C. For image analysis, cells were imaged using a Zeiss Axiovert 200 M fluorescence microscope (Carl Zeiss, Germany). All laser intensities used to detect the same immunostained markers were the same and all laser intensities used for capturing images were not saturated. Images were exported as .tif files using Zeiss Axioversion 4.8 and processed using Adobe Photoshop version 7.0 software.

2.5 Enzyme-linked immunosorbent assay (ELISA) analysis of plasma

The detailed ELISA procedure has been described in our previous publication.[18] EIA polystyrene microtiter plates were coated with 50 μg of the protein lysate sample and incubated at 37 °C for 2 h. The plate was washed three times with phosphate buffered saline with Tween-20 (PBS-T) and three times with PBS. Plates were then blocked with 100 μL of 5% skimmed milk in PBS at 37 °C for 2 h and then washed three times with PBST. Antibody solution was added and incubated at 37 °C for 2 h. After washing with PBST and PBS 10 times in total, 100 μL of peroxidise-conjugated secondary antibody in PBS was added for incubation at 37 °C for 2 h. Following 10 washes, 100 μL of 3,3′,5,5′-tetramethyl benzidine (Pierce) was added. After incubation at room temperature for 30 min, 100 μL of 1 M H_2SO_4

was added to stop the reaction and the absorbance at 450 nm measured using a Stat Fax 2100 microtiter plate reader (Awareness Technology Inc. FL, USA).

2.6 Sample preparation for 2D-DIGE experiment, gel image analysis, protein staining, in-gel digestion and MALDI-TOF MS analysis

MCF-7 and MDA-MB-231 cells treated with individual IC_{50} concentrations of rhein in complete cell culture medium for 24 h or treated with vehicle (DMSO, 0.1% (w/v) in media), were washed twice in 0.5× PBS, drained well and lysed in 2-D lysis buffer containing 4% w/v CHAPS, 7 M urea, 2 M thiourea, 10 mM Tris-HCl pH 8.3 and 1 mM EDTA. The detailed experimental procedures have been described in our previous study.[16,17,19] Notably, peaks in the mass range of *m*/*z* 800–3000 were used to generate a peptide mass fingerprint that was searched against the Swiss-Prot/TrEMBL database (v57.12) with 513877 entries using Mascot software v2.2.06 (Matrix Science, London, UK). The following parameters were used for the search: *Homo sapiens*; tryptic digest with a maximum of 1 missed cleavage; carbamidomethylation of cysteine, partial protein N-terminal acetylation, partial methionine oxidation and partial modification of glutamine to pyroglutamate and a mass tolerance of 50 ppm. Identification was accepted based on significant MASCOT Mowse scores ($p < 0.05$), spectrum annotation and observed *versus* expected molecular weight, and p*I* on 2-DE as well as at least 5 peptides in each identified protein.

For redox DIGE analysis, cells were lysed in 2-DE buffer (4% w/v CHAPS, 8 M urea, 10 mM Tris-HCl pH 8.3 and 1 mM EDTA) in the presence of ICy3 or ICy5 (80 pmol per mg protein) on ice to limit post-lysis thiol modification. Test samples were labeled with the ICy5 dye and mixed with an equal amount of a standard pool of both samples labeled with ICy3. Since ICy dyes interfered with the protein assay, protein concentrations were determined on replica lysates not containing dye. Lysates were left in the dark for 1 h followed by labeling with Cy2 to monitor the protein level The reactions were quenched with DTT (65 mM final concentration) for 10 min followed by L-lysine (a 20-fold molar ratio excess of free L-lysine to Cy2 dye) for a further 10 min. Volumes were adjusted to 450 μL with buffer plus DTT and IPG buffer for rehydration. All samples were run in triplicate against the standard pool.

2.7 Immunoblotting analysis

Immunoblotting analysis was used to validate the differential abundance of mass spectrometry identified proteins as well as determine the protein expression in cells. The detailed experimental procedures were described in our previous reports.[10,20,21] Briefly, cells were lysed with a lysis buffer containing 50 mM HEPES pH 7.4, 150 mM NaCl, 1% NP40, 1 mM EDTA, 2 mM sodium orthovanadate, 100 μg mL^{-1} AEBSF, 17 μg mL^{-1} aprotinin, 1 μg mL^{-1} leupeptin, 1 μg mL^{-1} pepstatin, 5 μM fenvalerate, 5 μM BpVphen and 1 μM okadaic acid prior to protein quantification with Coomassie Protein Assay Reagent (BioRad). 30 μg of protein samples were diluted in Laemmli sample buffer (final concentrations: 50 mM Tris pH 6.8, 10% (v/v) glycerol, 2% SDS (w/v), 0.01% (w/v) bromophenol blue) and separated by 1D-SDS-PAGE following standard procedures. After transferring separated proteins onto 0.45 μm Immobilon P membranes (Millipore), the membranes were blocked with 5% w/v skim milk in TBST (50 mM Tris pH 8.0, 150 mM NaCl and 0.1% Tween-20 (v/v)) for 1 h. Membranes were incubated in primary antibody solution in TBS-T containing 0.02% (w/v) sodium azide for 2 h. Membranes were washed in TBS-T (3 × 10 min) and then probed with the appropriate horseradish peroxidase-coupled secondary antibody (GE Healthcare). After washing in TBS-T 6 times (15 min each), immunoprobed proteins were visualized using an enhanced chemiluminescence method (Visual Protein Co.).

2.8 Assay for endogenous reactive oxygen species using DCFH-DA

MCF-7 and MDA-MB-231 cells (10 000 cells per well) were incubated with the indicated concentrations of rhein for 20 min. After two washes with PBS, cells were treated with 10 μM of 2,7-dichlorofluorescin diacetate (DCFH-DA; Molecular Probes) at 37 °C for 20 min, and subsequently washed with PBS. Fluorescence was recorded at an excitation wavelength of 485 nm and an emission wavelength of 530 nm.

2.9 Assay for the effect of *N*-acetylcysteine on rhein-induced cell death

To examine the effect of an antioxidant, *N*-acetylcysteine (NAC), on rhein-induced cell death, cells were pretreated with NAC (10 and 20 mM) or vehicle (PBS) for 3 h before the treatment with indicated concentrations of rhein for 24 h or left untreated. After removal of the medium, 50 μL of MTT working solution (1 mg mL^{-1}) (Sigma) was added to the cells in each well, followed by a further incubation at 37 °C for 4 h. The supernatant was carefully removed. 100 μL of DMSO was added to each well and the plates shaken for 20 min. The absorbance of samples was then measured at 540 nm in a multi-well plate reader. Values were normalized against the untreated samples and were averaged from 4 independent measurements.

2.10 Validation of thiol reactivity changes by immunoprecipitation coupled to immunoblotting

Rhein treated MCF-7 and MDA-MB-231 cells were lysed in the presence of ICy3 or ICy5 dyes to limit post-lysis thiol modification. The labeling reactions were performed in the dark at 37 °C for 1 h and then quenched with a 2-fold molar excess of DTT for 10 min. 500 μg of ICy dye-labeled cell lysate was then diluted 20-fold with NP40 buffer containing protease inhibitors and then incubated with 5 μg primary antibody and 40 μL of a 50% slurry of protein A-Sepharose for 16 h at 4 °C. Immune complexes were then washed three times in lysis buffer and boiled in Laemmli sample buffer prior to resolving by SDS-PAGE. ICy images were scanned directly between low-fluorescence glass plates using an Ettan DIGE Imager (GE Healthcare) followed by immunoblotting analysis with the same primary antibody to detect the specific protein. The immunoblotting procedure is described above.

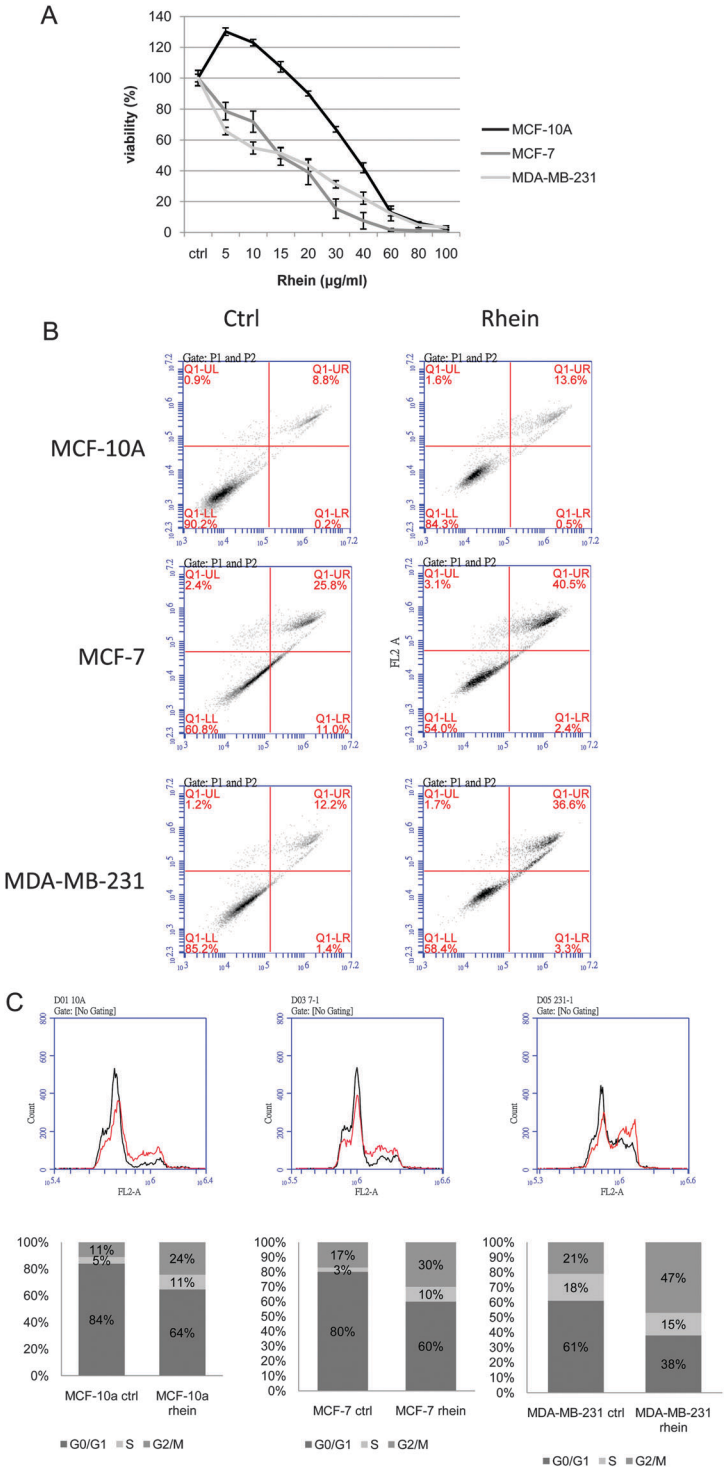

Fig. 1 Rhein-induced loss of cell viability, increased cell apoptosis and blocked cell cycle progression in MCF-10A cells, MCF-7 cells and MDA-MB-231 cells. (A) MTT-based viability assays were performed on MCF-10A cell, MCF-7 cell and MDA-MB-231 cell cultures. Values from rhein-treatments were normalized against individual untreated control groups and were the average of 6 independent measurements +/− the standard deviation. (B) 10^6 MCF-10A cells, MCF-7 cells and MDA-MB-231 cells treated with/without 15 μg mL^{-1} rhein were incubated with Alexa Fluor 488 and propidium iodide in 1× binding buffer at room temperature for 15 min, and then stained cells were analyzed by flow cytometry to examine the effect of rhein-treatment on apoptosis in MCF-10A cells, MCF-7 cells and MDA-MB-231 cells. Annexin V is presented on the *x*-axis as FL1-H, and propidium iodide is presented on the *y*-axis as FL2-H. LR quadrant indicates the percentage of early apoptotic cells (Annexin V positive cells), and UR quadrant indicates the percentage of late apoptotic cells (Annexin V positive and propidium iodide positive cells). (C) Cell-cycle analysis using propidium iodide staining. The *y*-axis shows the intensity of PI, and the *x*-axis shows the number of cells. The black lines display the full length DNA of control MCF-10A cells, MCF-7 cells and MDA-MB-231 cells; in contrast, the red lines display the full length DNA of rhein-treated MCF-10A cells, MCF-7 cells and MDA-MB-231 cells (upper panels). The G0/G1 phase, S phase and G2/M phase distributions of vehicle-treated and rhein-treated MCF-10A cells, MCF-7 cells and MDA-MB-231 cells (bottom panels).

2.11 Flow cytometry analysis for apoptosis detection

Annexin-V/propidium iodide (PI) double assay was performed using the Annexin V, Alexa Fluor® 488 Conjugate Detection kit (Life technologies). Following rhein treatment, cells were trypsinized from culture dish and washed twice with cold PBS. 1×10^6 cells were resuspended in 500 μL binding buffer and stained with 5 μL Alexa Fluor 488 conjugated annexin V according to the manufacturer's instructions. 1 μL 100 μg mL^{-1} propidium iodide (PI) was added and mixed gently to incubate with cells for 15 min at room temperature in the dark. After the incubation period, samples were subjected to FCM analysis in 1 h using BD Accuri C6 Flow Cytometry (BD Biosciences, San Jose, CA). The data were analyzed using Accuri CFlow@ and CFlow Plus analysis software (BD Biosciences).

3. Results

3.1 Rhein induces cell death and cell apoptosis in MCF-10A cells, MCF-7 cells and MDA-MB-231 cells

Our previous study demonstrated that rhein is able to inhibit cell proliferation in both HER2 overexpression and HER2-basal expression in breast cancer cells.[22] In the current study, rhein has been shown to be less toxic to non-tumorigenic MCF-10A breast cells in comparison to non-invasive breast cancer cells, MCF-7, and invasive breast cancer cells, MDA-MB-231 (Fig. 1). To evaluate the effect of rhein on breast cancer cells, we exposed MCF-10A cells, MCF-7 cells and MDA-MB-231 cells to a dose range (0–100 μg mL^{-1}) of rhein for 24 h and performed MTT assays. Exposure of MCF-7 cells and MDA-MB-231 cells to rhein were shown to result in a dose-dependent loss of cell viability. At a rhein concentration of 15 μg mL^{-1}, a significant loss of cell viability (50%) was detectable after 24 h. In contrast, non-tumorigenic MCF-10A breast cells were shown to have a higher IC_{50} value at 35 μg mL^{-1} demonstrating that rhein is less toxic for non-tumorigenic breast cells rather than for breast cancer cells (Fig. 1A). In order to verify rhein-induced breast cancer cell toxicity, we also examined the changes of cell apoptosis in MCF-10A cells, MCF-7 cells and MDA-MB-231 cells treated with 15 μg mL^{-1} of rhein for 24 h. We used flow cytometry with propidium iodide staining and annexin V-conjugated Alexa Fluor 488 to analyze the percentages of apoptotic MCF-10A cells, MCF-7 cells and MDA-MB-231 cells treated with/without 15 μg mL^{-1} of rhein. The experimental data indicated that treatment of rhein increases the percentages of total apoptotic cells in MCF-10A cells, MCF-7 cells and MDA-MB-231 cells by 5.0%, 11% and 26.3%, respectively. Notably, most of these apoptotic events were taking place in the late apoptotic stage where the apoptotic rates were increased for 4.8%, 14.7% and 24.4% in MCF-10A cells, MCF-7 cells and MDA-MB-231 cells, respectively. These results imply that rhein induces more significant cell apoptosis in non-invasive breast cancer cells, MCF-7, as well as in invasive breast cancer cells, MDA-MB-231, rather than in non-tumorigenic MCF-10A breast cells and most of these apoptosis events are involving late apoptotic stage (Fig. 1B). Further analysis of cell

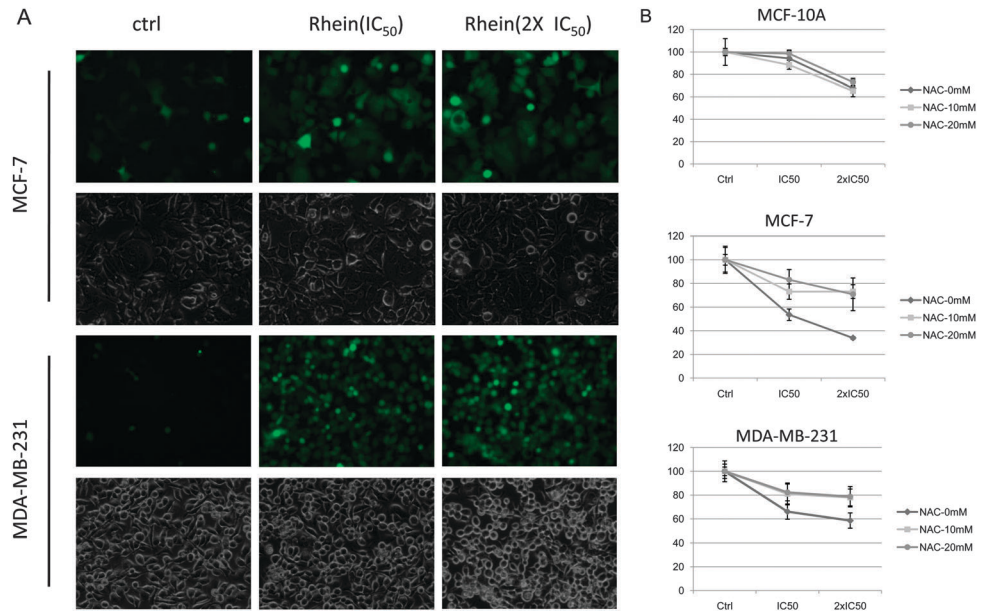

Fig. 2 Effect of rhein on MCF-7 and MDA-MB-231 ROS production. (A) DCFH-based intracellular ROS production assays were performed where 10 000 MCF-7 and MDA-MB-231 cells were plated onto 96-well plates in medium containing 10% FBS. After 24 h, the cells were treated with the indicated concentrations of rhein for a further 24 h. Cells were then treated with 10 μM of DCFH-DA at 37 °C for 20 min and the fluorescence images were recorded at excitation and emission wavelengths of 485 nm and 530 nm, respectively. Each set of three fields was taken using the same exposure, and images are representative of three different fields. (B) Effect of pretreatment of NAC (10 mM and 20 mM) or vehicle (PBS) on rhein-induced cell death in MCF-10A, MCF-7 and MDA-MB-231 cells. Cells were treated with varying concentrations of rhein (0, 1 × IC_{50} and 2 × IC_{50}) for 24 h and then harvested for analysis of cell viability using the MTT assay as detailed in Materials and methods.

cycle distributions by flow cytometry revealed that rhein can significantly induce G2/M cell-cycle arrest in both MCF-7 cells and MDA-MB-231 cells rather than in MCF-10A cells (Fig. 1C).

3.2 Rhein induces generation of intracellular ROS in MCF-7 cells and MDA-MB-231 cells

Previous reports have shown that rhein is able to induce apoptosis in human prostate and colon cancer cells through the generation of ROS.[23] However, few studies of this in breast cancer cells have been reported. Accordingly, we tested the hypothesis whether rhein-induced cell death in breast cancer is initiated through ROS generation. Using DCF fluorescence as readout, treatment of MCF-7 and MDA-MB-231 cells with $1 \times IC_{50}$ or $2 \times IC_{50}$ concentrations of rhein for 20 min resulted in a dose-dependent increase in ROS generation compared with untreated MCF-7 and MDA-MB-231 cells (Fig. 2A). We further

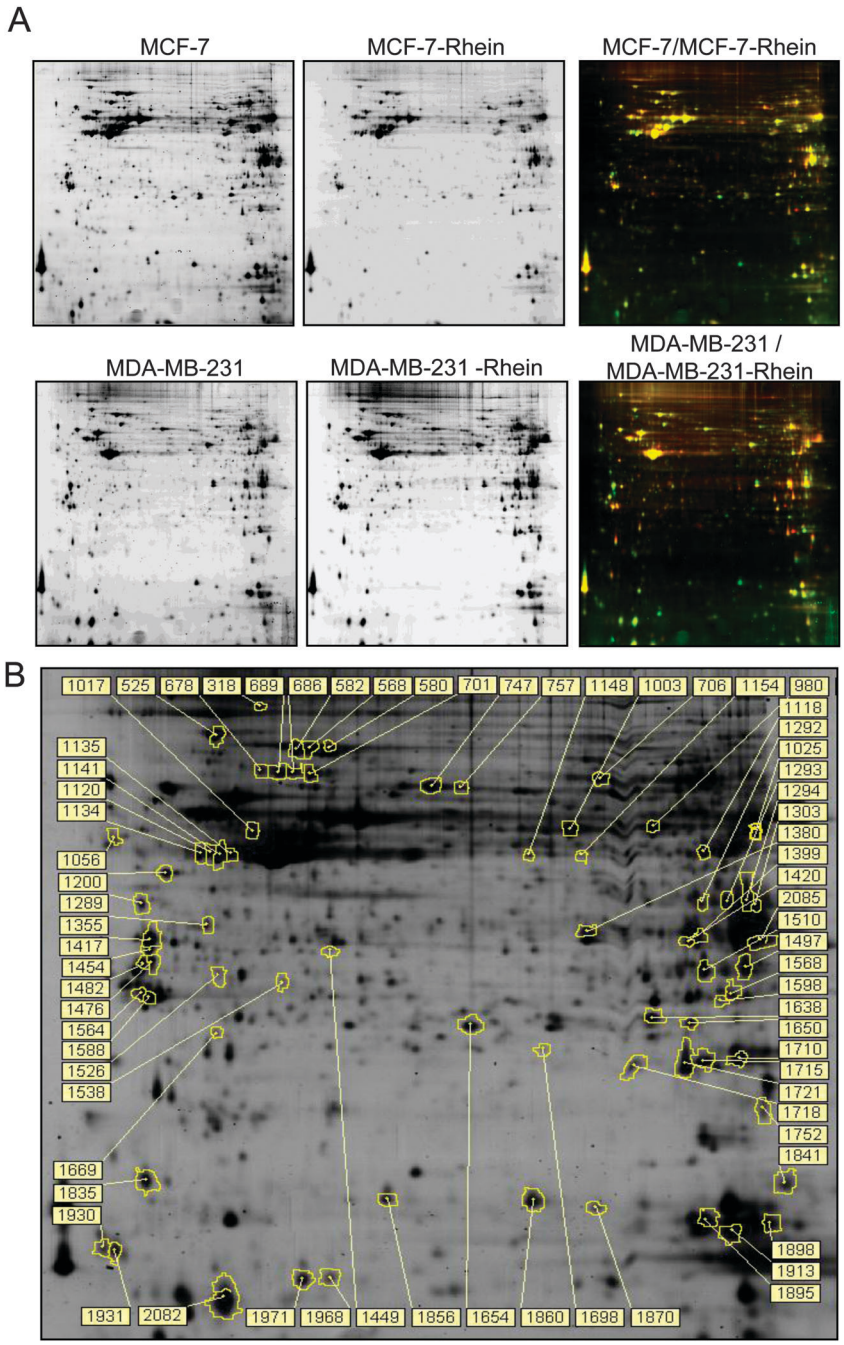

Fig. 3 2D-DIGE analysis of rhein-induced differential protein expression in MCF-7 cells and MDA-MB-231 cells. (A) MCF-7 cells and MDA-MB-231 cells were treated with an IC_{50} concentration of rhein for 24 h or left untreated. Lysates were prepared in triplicate and 2D-DIGE analysis performed according to Materials and methods. 2D-DIGE images of the protein samples from untreated and rhein-treated MCF-7 cells and MDA-MB-231 cells are displayed, respectively. (B) Identified differentially expressed protein features are annotated with spot numbers.

checked whether a cell-permeable anti-oxidant could rescue cells from rhein-induced cell death due to the generation of ROS. The result demonstrated that pretreatment with NAC offered significant protection against rhein-induced cell death in both MCF-7 and MDA-MB-231 cells at each dose of rhein. On the other hand, the pretreatment of NAC had no significant effect on MCF-10A cells (Fig. 2B).

3.3 2D-DIGE and MALDI-TOF MS analysis of rhein-induced proteomic alterations in MCF-7 cells and MDA-MB-231 cells

In order to analyze rhein-induced proteomic alterations, MCF-7 cells and MDA-MB-231 cells were grown on cell culture dishes prior to treatment with an IC_{50} concentration (15 μg mL^{-1}) of rhein or treated with a vehicle. Three biological replicates for each treatment were compared by 2D-DIGE to provide a global overview of rhein-induced differential protein expression. Image analysis revealed more than 2094 well-defined protein features (Fig. 3A). Those appearing in all replicates and showing a change in average abundance of >1.5-fold ($P < 0.05$) between the treated and untreated cell lysates were excised from gels for protein identification. MALDI-TOF MS as well as MALDI-TOF/TOF MS identification revealed 34 and 60 differentially expressed proteins between rhein-treated and untreated MCF-7 cells and MDA-MB-231 cells, respectively (Fig. 3B, Fig. S1 and Table S1, ESI†). More than half of the differentially expressed proteins identified were cytosolic proteins

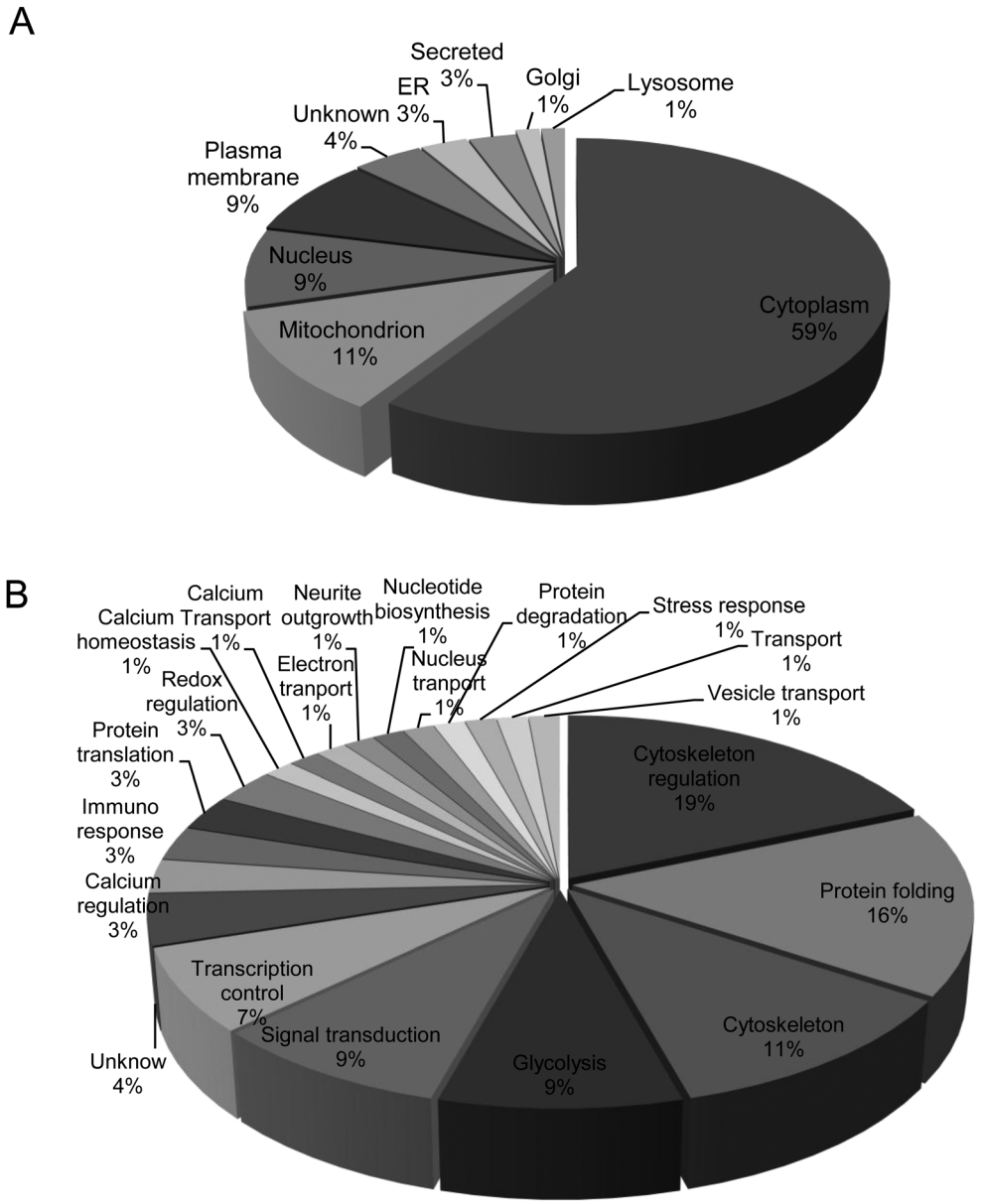

Fig. 4 Distribution of differentially expressed proteins from rhein-treated and untreated MCF-7 cells and MDA-MB-231 cells according to (A) the subcellular location and (B) biological function.

(Fig. 4A) and predominantly involved in cytoskeleton regulation, protein folding, cytoskeleton, glycolysis, signal transduction and transcription control (Fig. 4B).

Using functional information from the Swiss-Prot and KEGG pathway databases, numerous biological functions were ascribed to the identified proteins with possible roles in rhein-induced cytotoxicity. Fig. 5 compares the expression profiles of the differentially expressed proteins. Proteins known to regulate protein folding, cytoskeleton regulation and glycolysis were found to be down-regulated in both rhein-treated MCF-7 cells and MDA-MB-231 cells.

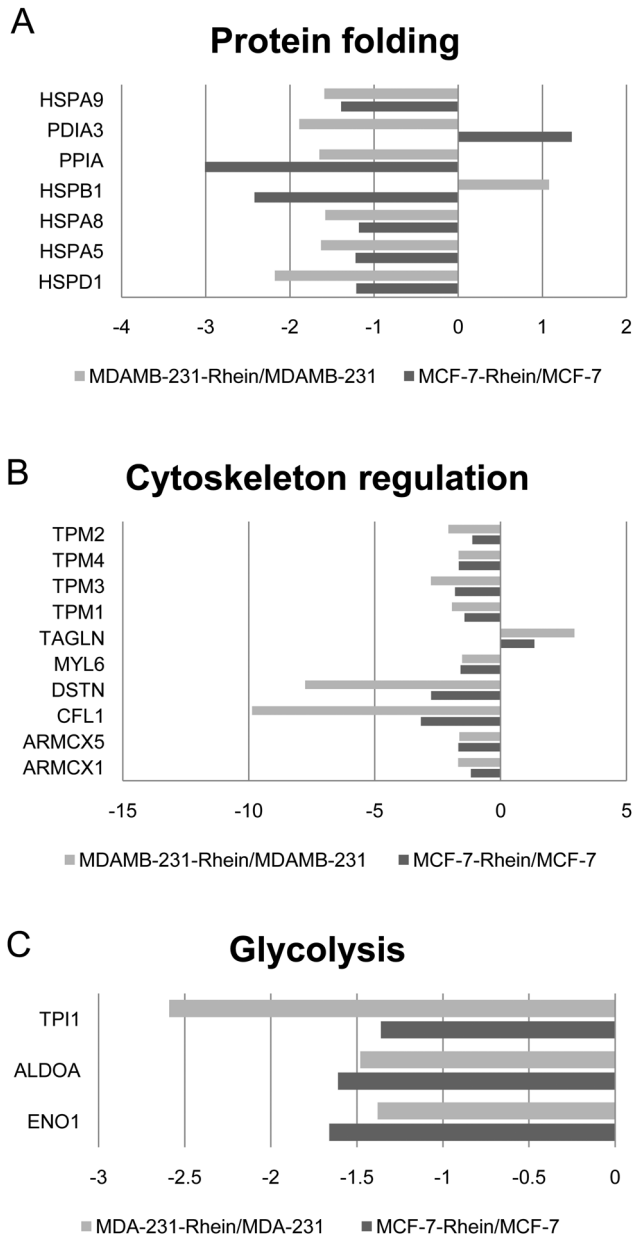

Fig. 5 Expression profiles for differentially expressed proteins potentially contributing to: (A) protein folding, (B) cytoskeleton regulation and (C) glycolysis. Horizontal bars represent fold-changes in protein expression in rhein-treated *versus* untreated MCF-7 cells and MDA-MB-231 cells for each protein. Additional details for each protein can be found in Table S1 (ESI†).

3.4 Validation of proteomic results by immunoblotting, immunofluorescence and ELISA

To validate differential expression of the identified proteins, immunoblotting, immunofluorescence and ELISA were performed to compare the protein expression levels between rhein- and vehicle control-treated MCF-7 and MDA-MB-231 cells. In general, there was a good correlation between changes observed in the 2D-DIGE analysis and by immunoblotting/immunofluorescence/ELISA analysis. Validation confirmed the expression levels of cathepsin D, galectin-3, HSP-27, tropomyosin alpha-4 and destrin by either immunoblotting or ELISA in MCF-7 cells since these proteins play essential roles in the regulation of cell physiology (Fig. 6). In addition, validation also confirmed the levels of 78 kDa glucose-regulated protein, annexin A3, SCaMC-3, cofilin-1, galectin-1, cytoskeletal 18, nucleobindin-1, peptidyl-prolyl *cis–trans* isomerase A, peroxiredoxin-1, protein disulfide-isomerase A3, stress-induced-phosphoprotein 1, tropomyosin alpha-1, cytoskeletal 19 and 60 kDa heat shock protein in MDA-MB-231 cells by immunoblotting, immunofluorescence or ELISA (Fig. 7).

3.5 Relationship between rhein and ER-stress

ROS have emerged as major regulators of ER function as well as unfolded protein response. The over-production of ROS has been evidenced to induce ER-stress which induces cellular dysfunction and cell death.[24] In the current study, we found that a number of cellular proteins coming from MCF-7 and MDA-MB-231 cells with their biological functions in protein folding such as 78 kDa glucose-regulated protein and redox-regulation such as peroxiredoxin-1 were significantly modulated in protein expression during rhein treatment implying that rhein might induce breast cancer apoptosis through misfolding of cellular proteins as well as unbalancing of the cellular redox status *i.e.* ER stress (Table S1, ESI†). In order to prove this hypothesis, ER-stress has been determined and the results indicated that rhein promotes ER-stress through the upregulation of ER-stress markers, ERO1L, GRP78, PERK, IRE1-α and calnexin. Importantly, compared with rhein-pretreated MCF-7 and MDA-MB-231 cells, ER-stress was insignificant in rhein-pretreated MCF-10A cells (Fig. 8).

3.6 Redox proteomic analysis of rhein-induced cysteine modifications of MCF-7 and MDA-MB-231 proteins

Rhein has been reported to induce cytotoxicity *via* ROS generation in several different cancer cell lines[23] and we also confirm ROS generation in MCF-7 and MDA-MB-231 cells (Fig. 2). We thus hypothesized that rhein-induced ROS might damage or deregulate cellular proteins by oxidative modification of their cysteinyl thiol groups. Accordingly, we applied a recently developed redox 2D-DIGE methodology utilizing iodoacetylated ICy dyes[25] to assess rhein-induced changes in protein thiol reactivity. Rhein-treated (15 μg mL^{-1}) or vehicle-treated cells were lysed in the presence of ICy5 in triplicate. Individual ICy5-labeled samples were then run on 2D gels against an equal load of ICy3-labeled standard pool comprising of an equal mixture of

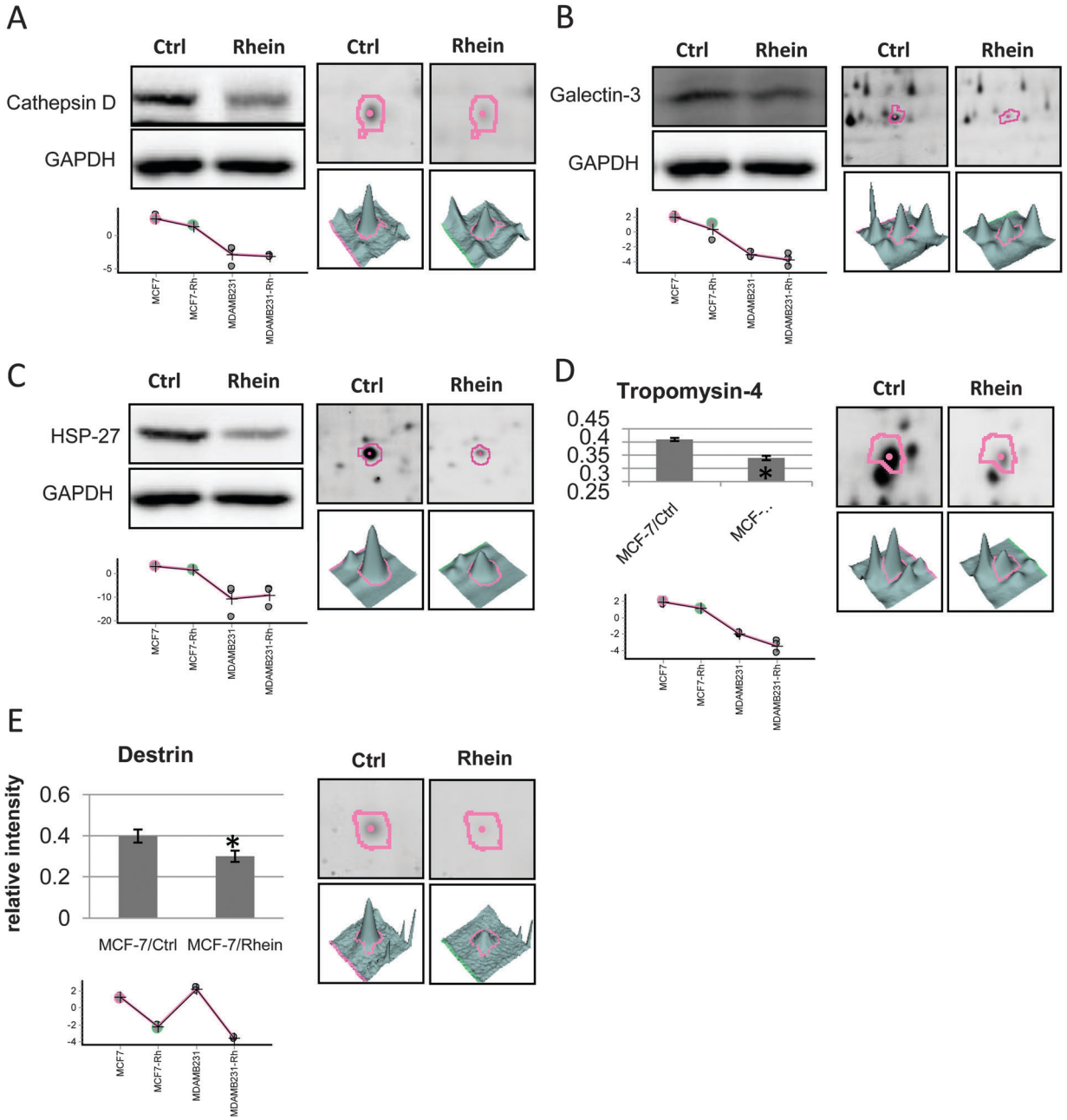

Fig. 6 Validation of rhein-induced differential protein expression in MCF-7 cells by immunoblotting and enzyme-linked immunosorbent assay. The altered expression of identified proteins; (A) cathepsin D, (B) galectin-3 and (C) HSP-27 were assessed by immunoblotting (left panels), while ELISA analysis was performed to determine the levels of (D) tropomyosin alpha-4 and (E) destrin in rhein-treated *versus* untreated MCF-7 cells (left panels). The protein 2D-DIGE map (right top panels) and three-dimensional spot image (right bottom panels) are also shown.

both sample types to aid in spot matching and to improve the accuracy of quantification. The ICy5-labeled samples were subsequently labeled with the lysine labeling Cy2 dye as an internal protein level control which was used to normalize the corresponding ICy5/ICy3 signals. 1343 protein features were detected, of which 242 displayed statistically significant differences in labeling due to rhein treatment (Fig. 9). CCB post-staining and matching with fluorescence images allowed confident picking of 129 gel features and 9 of these were identified as unique gene products by MALDI-TOF peptide mass fingerprinting (Table S2, ESI† and Fig. 9). All of the identified proteins contain at least one cysteine, and since the ICy dyes target reduced cysteinyl thiols, these results suggest that rhein alters the oxidative status of some of these thiol groups. The possible biological roles of these modifications are discussed below and warrant further investigation. The differentially labeled proteins were mostly

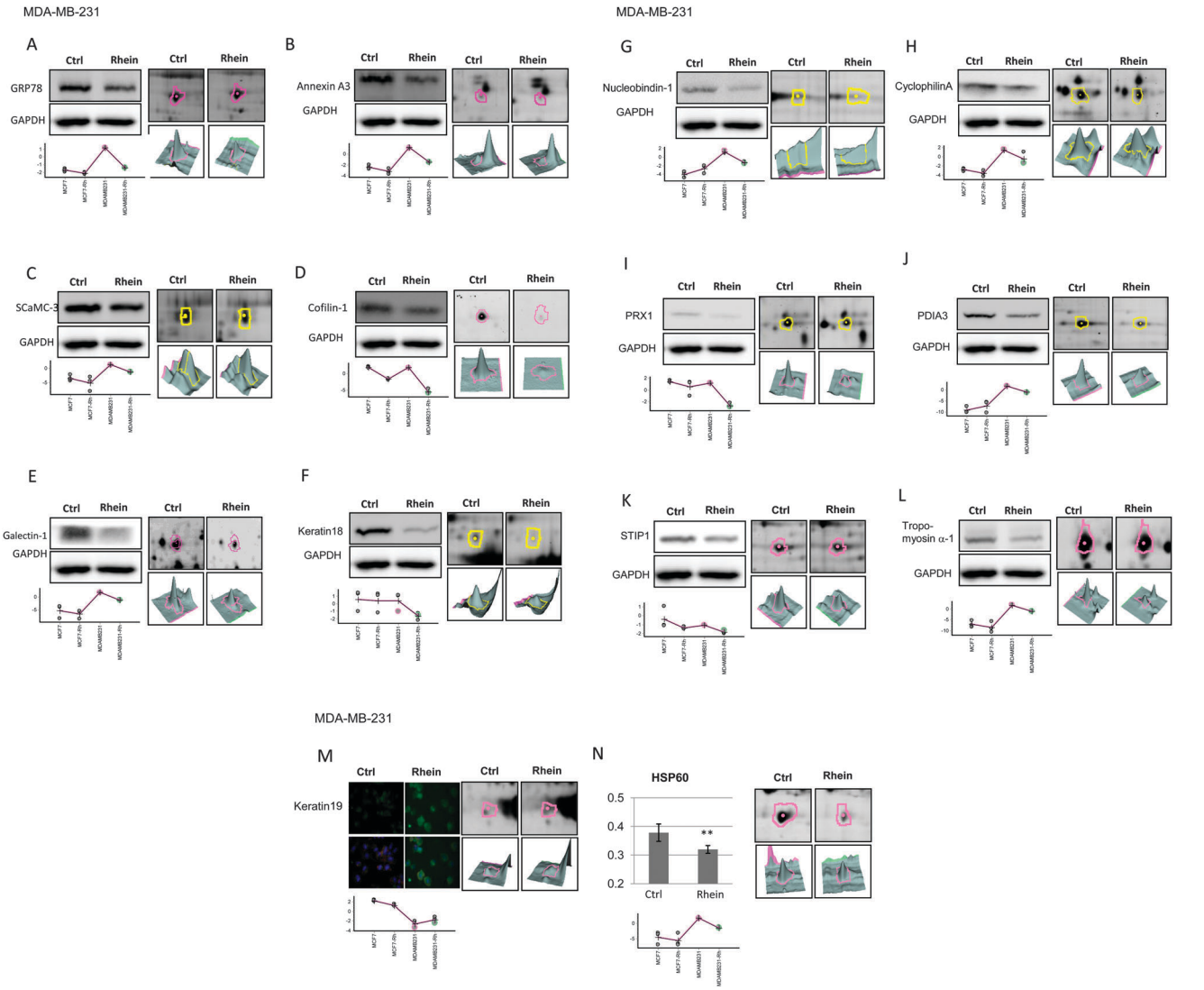

Fig. 7 Validation of rhein-induced differential protein expression in MDA-MB-231 cells by immunoblotting, immunofluorescence and ELISA. The altered expression of identified proteins; (A) 78 kDa glucose-regulated protein, (B) annexin A3, (C) SCaMC-3, (D) cofilin-1, (E) galectin-1, (F) cytoskeletal 18, (G) nucleobindin-1, (H) peptidyl-prolyl *cis–trans* isomerase A, (I) peroxiredoxin-1, (J) protein disulfide-isomerase A3, (K) stress-induced-phosphoprotein 1 and (L) tropomyosin alpha-1 were assessed by immunoblotting (left panels), while immunofluorescence analysis and ELISA analysis were performed to determine the levels of (M) cytoskeletal 19 and (N) 60 kDa heat shock protein in rhein-treated *versus* untreated MDA-MB-231 cells (left panels), respectively. The protein 2D-DIGE map (right top panels) and three-dimensional spot image (right bottom panels) are also shown.

cytoplasmic and fell into several functional groups including cytoskeleton regulation, protein translation, immuno response, protein folding, redox regulation and glycolysis (Table S2, ESI†).

3.7 Validation of redox-induced changes in peroxiredoxin-2

To validate alterations of thiol reactivity of the identified proteins, immunoprecipitation combined with immunoblotting was performed to compare the free thiol group levels and protein expression levels between rhein- and control-treated MCF-7 cells. In here, we choose one of the most significant change proteins, peroxiredoxin-2, to validate the thiol reactive alterations on this protein. Validation result confirmed the increase of free thiol content of peroxiredoxin-2 and no significant change of the protein level in rhein-treated MCF-7 cells compared to untreated cells (Fig. 10).

4. Discussion

Extensive attention has been paid to the identification of naturally occurring chemotherapeutic botanicals which are able to inhibit, delay or reverse tumorigenesis or metastasis. The assessment of ancient herbal medicines might offer an approach for the treatment of breast cancer, which remains a primary cause of cancer-related deaths all over the world.[26] In the present study, we examined the molecular mechanisms of rhein cytotoxicity in breast cancer cells *in vitro* since rhein has been shown to exhibit

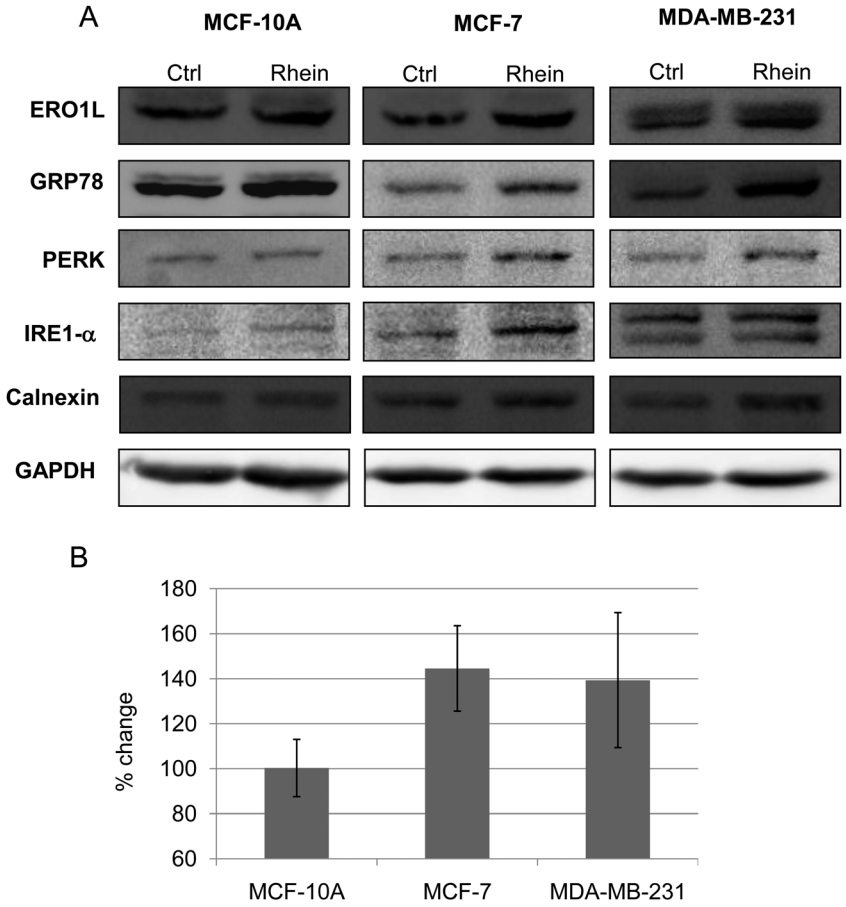

Fig. 8 Rhein-induced increase in ER-stress in MCF-7 cells and MDA-MB-231 cells. (A) The levels of ER-stress proteins, ERO1L, GRP78, PERK, IRE1-α and calnexin were confirmed by immunoblot analysis. (B) The statistical analysis of rhein-induced alterations against untreatment of these ER-stress proteins was displayed.

anti-tumorigenic ability in several different cancer types.[27,28] By means of 2D-DIGE and MALDI-TOF MS, more than 70 rhein-induced alterations in protein expression have been identified in either MCF-7 or MDA-MB-231 cells. The results demonstrate that this strategy is powerful enough to identify a broad-ranging signature of rhein-induced cytotoxicity, with the altered proteins having roles in cytoskeleton regulation, protein folding, cytoskeleton, glycolysis, signal transduction and transcription control. Even though the global coverage of protein mixtures identified by LC-MS based analysis is generally recognized to be higher than that of 2-DE based analysis, 2-DE based analysis offers the advantage of direct protein quantification at the protein isoform level with reduced analytical variation.[9] Our study also revealed that treatment of breast cancer cells with rhein results in the generation of reactive oxygen species. Since ROS can activate signaling pathways, modulate a variety of cellular activities and regulate disease progression, it is important to study the molecular events associated with their effects. Accordingly, our previously established cysteine-labeling 2D-DIGE platform using ICy3/ICy5 dyes was thus used to determine if protein thiol reactivity is altered in cells following treatment with rhein due to ROS generation.

Our previous studies using MCF-7 cells as an *in vitro* model revealed that treatment with rhein results in decreased cell viability at least partially through the over-expression of p21, caspase-9 and ASK1 expression.[22] In addition, current proteomic analysis revealed that heterogeneous nuclear ribonucleoprotein K and heterogeneous nuclear ribonucleoproteins A2/B1, key eukaryotic mRNA processing proteins, were down-regulated in response to rhein treatment. Previous report demonstrated that down-regulated of heterogeneous nuclear ribonucleoprotein K mediating TRAIL-induced apoptosis and reducing FLIP-involved anti-apoptotic activity.[29] Additionally, down-regulation of heterogeneous nuclear ribonucleoproteins A2/B1 leads to the increased formation of pro-apoptotic Bcl-x(s) and promoted apoptosis of BxPc3 cells.[30] Thus, the down-regulation of heterogeneous nuclear ribonucleoprotein K and heterogeneous nuclear ribonucleoproteins A2/B1 may contribute to rhein-induced apoptosis of breast cancer cells through inactivation of mRNA processing. Another identified rhein-induced down-regulated protein was galectin-3, which has been reported to promote cancer cell proliferation and suppress cancer cell apoptosis.[31,32] Galectin-3 was previously shown to modulate CD95, a member of the tumor necrosis factor family, and inhibit the apoptotic signaling pathway.[33] Overexpression of galectin-3 has been evidenced to prevent bladder carcinoma cells from TRAIL-induced apoptosis through constitutive activation of Akt, whereas blockage of the

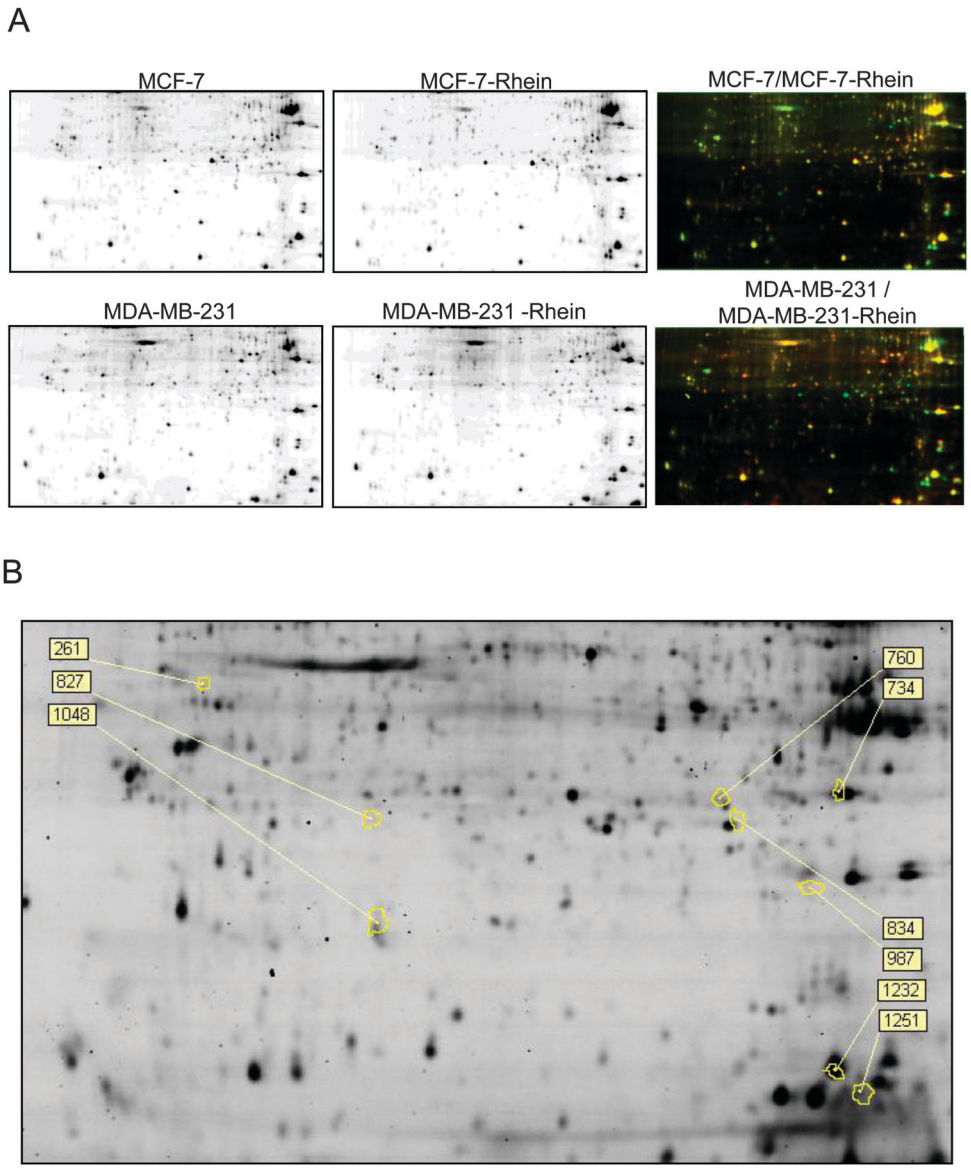

Fig. 9 Redox 2D-DIGE analysis of rhein-induced differential cysteine-modification in MCF-7 cells and MDA-MB-231 cells. (A) Lysates from MCF-7 cells and MDA-MB-231 cells treated with 15 μg mL^{-1} of rhein or left untreated were subjected to redox 2D-DIGE analysis as described in Materials and methods. Images of protein samples from untreated and rhein-treated MCF-7 cells and MDA-MB-231 cells are displayed. (B) Identified differentially labeled protein features are annotated with spot numbers.

PI3K signaling pathway significantly reduced the protecting effect of galectin-3 on cell apoptosis suggesting that galectin-3 involves Akt as a modulator molecule in protecting bladder carcinoma cells from TRAIL-induced apoptosis.[34] Accordingly, the down-regulation of galectin-3 may contribute to rhein-induced apoptosis of breast cancer cells through inactivation of Akt and subsequent activation of TRAIL-related apoptosis.

Our proteomic analysis revealed rhein to down-regulate the majority of identified proteins which are involved in a variety of cellular processes including protein folding, cytoskeleton regulation and glycolysis (Fig. 5). We hypothesize that rhein may interfere with the proper folding of cellular proteins through the reduced expression of folding and protein chaperones such as 60 kDa heat shock protein, 78 kDa glucose-regulated protein, heat shock cognate 71 kDa protein, heat shock protein beta-1, peptidyl-prolyl *cis–trans* isomerase A, protein disulfide-isomerase A3 and mitochondrial stress-70 protein and that this may be linked to a general stress response as well as ER stress response. Importantly, peptidyl-prolyl *cis–trans* isomerase A has been reported to be able to inactivate procaspase-3 activity through sequestering cytochrome *c*.[35] Accordingly, it is tempting to consider that rhein might trigger apoptosis of MCF-7 and MDA-MB-231 cells at least partially through the down-regulation of peptidyl-prolyl *cis–trans* isomerase A. Mitochondria are well-defined to play a major role in regulating cellular apoptosis[36] and recent reports indicate that rhein inhibits mitochondrial electron transport[37] and induces apoptosis through a mitochondria/caspase-dependent pathway in human kidney cells.[38] The deregulation of mitochondrial

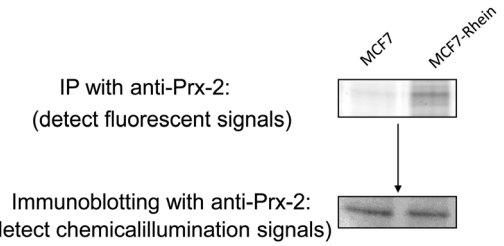

Fig. 10 Validation of the thiol reactive protein, peroxiredoxin-2, identified through a redox-proteomic study in MCF-7 cells after rhein treatment by IP-WB. ICy dye-labeled protein samples from MCF-7 cells were either untreated or treated with 15 μg mL^{-1} of rhein followed by immunoprecipitation with anti-peroxiredoxin-2 antibody to confirm the alterations of thiol reactivity in peroxiredoxin-2. The image was visualized by Ettan DIGE imager. Immunoblotting against the corresponding antibody was performed to gain the protein level.

electron transport proteins in the current study appears to support this.

Particularly, all of the identified proteins with roles in cellular metabolism (mainly glycolytic enzymes) were found to be down-regulated, implying relationship between rhein-induced apoptosis and cellular metabolism in breast cancer. In fact, it has been previously revealed that BAD, a member of pro-apoptotic Bcl-2 family, exists in a glucokinase-containing complex in the mitochondrion that modulates glucose-dependent mitochondrial respiration and cell death dependent upon glucose availability.[39,40] Consequently, rhein might deregulate glycolysis in both MCF-7 and MDA-MB-231 cells *via* its effect on pro-apoptotic proteins such as BAD. Notably, the identified glycolytic enzymes including triosephosphate isomerase, fructose-bisphosphate aldolase A and alpha-enolase displayed significant down-regulation, also supporting previous data demonstrating that oxidative stress can redirect carbohydrate fluxes to generate increased reducing power in the form of NADPH at the expense of glycolysis.[41,42]

Rhein has been reported to induce ROS which are essential mediators of attenuated tumor growth and cancer cell apoptosis.[8] These processes are mediated by increasing endoplasmic reticulum stress, blocking the G2/M checkpoint, reducing mitochondrial potential, promoting the expression of caspases and activation of JNK and p38 MAPK signaling pathways. Our present data support these observations that rhein can induce cell death in MCF-7 and MDA-MB-231 cells through the generation of ROS and the G2/M transition.

ROS are known to modify protein cysteinyl thiol groups, resulting in oxidative damage.[43–45] We therefore applied a recently developed 2D-DIGE methodology utilizing iodoacetyl ICy dyes to assess rhein-induced changes in the thiol reactivity of cellular proteins in MCF-7 cells and MDA-MB-231 cells. Individual ICy5- and Cy2-labeled samples were run on 2D gels against an equal load of an ICy3-labeled standard pool consisting of an equal mixture of the differentially treated samples to accurately determine changes in the thiol reactivity of the proteins. This experimental design accurately quantified changes in the thiol reactivity of cysteine residues taking into consideration variation due to protein expression change.

The ICy labeling data presented support the hypothesis that rhein can induce the formation of free thiols in certain proteins through disruption of disulphide bonds; meanwhile, rhein induced ROS or protein-derived peroxides may directly oxidize thiol groups to form the sulfenic, sulfinic or sulfonic acid forms of cysteine, which would not react with the ICy dyes. These thiol modifications have been reported to perturb the normal functions of the proteins.[46] In the current study, 9 proteins with differential thiol reactivity were identified by MALDI-TOF MS. Peroxiredoxin-2, galectin-3, triosephosphate isomerase, peptidyl-prolyl *cis–trans* isomerase A and cofilin-1 are reported to maintain the cell redox status and protein folding as well as regulate glycolysis and cytoskeleton formation and all displayed an increase in ICy dye labeling following rhein treatment (Table S2, ESI†). Thus, their cysteine residues must be reduced to generate new thiol groups for ICy labeling, implying possible oxidative damage and deregulation of these proteins. In contrast, several of the identified proteins, such as elongation factor 1-delta, phosphoglycerate mutase 1, heat shock protein beta-1 and peroxiredoxin-1, displayed a decrease in ICy dye labeling following rhein treatment (Table S2, ESI†). Thus, their free thiol groups must be oxidized in response to rhein treatment to block ICy labeling, implying possible oxidative damage and deregulation of these proteins.

In conclusion, the present study offers an insight into the mechanisms of rhein-induced apoptosis in human breast cancer cells and shows a link between ROS generation and the cell death process. Further study also indicated that rhein promotes misfolding of cellular proteins as well as unbalancing of cellular redox status leading to ER-stress. The findings of this study may have clinical implications in that rhein treatment may be useful in destroying fast-growing cancer cells with limited toxicity to normal cells. Additionally, numerous identified cellular proteins may be useful for further evaluation as potential targets in breast cancer therapy.

Declaration of competing interests

The authors confirm that there are no conflicts of interest.

Abbreviations

2-DE	Two-dimensional gel electrophoresis
CCB	Colloidal coomassie blue
CHAPS	3-[(3-Cholamidopropyl)-dimethylammonio]-1-propanesulfonate
DCFH-DA	2,7-Dichlorofluorescin diacetate
ddH_2O	Double deionized water
DIGE	Differential gel electrophoresis
DTT	Dithiothreitol
EDTA	Ethylenediaminetetraacetic acid
FCS	Fetal calf serum
MALDI-TOF MS	Matrix assisted laser desorption ionization-time of flight mass spectrometry
NP-40	Nonidet P-40

SDS	Sodium dodecyl sulfate
TFA	Trifluoroacetic acid

Acknowledgements

This work was supported by NSC grant (100-2311-B-007-005, 101-2311-B-007-011 and NSC 102-2311-B-007-009) from National Science Council, Taiwan, and Toward World-Class University projects from National Tsing Hua University (101N2725E1, 101N2771E1 and 101N2051E1).

References

1 X. You, S. Feng, S. Luo, D. Cong, Z. Yu, Z. Yang and J. Zhang, *Fitoterapia*, 2013, **85**, 161–168.
2 X. Sheng, X. Zhu, Y. Zhang, G. Cui, L. Peng, X. Lu and Y. Q. Zang, *Int. J. Biol. Sci.*, 2012, **8**, 1375–1384.
3 Y. Zhang, S. Fan, N. Hu, M. Gu, C. Chu, Y. Li, X. Lu and C. Huang, *PPAR Res.*, 2012, **2012**, 374936.
4 Z. H. He, R. Zhou, M. F. He, C. B. Lau, G. G. Yue, W. Ge and P. P. But, *Phytomedicine*, 2011, **18**, 470–478.
5 D. K. Joung, H. Joung, D. W. Yang, D. Y. Kwon, J. G. Choi, S. Woo, D. Y. Shin, O. H. Kweon, K. T. Kweon and D. W. Shin, *Exp. Ther. Med.*, 2012, **3**, 608–612.
6 Y. Y. Chen, S. Y. Chiang, J. G. Lin, Y. S. Ma, C. L. Liao, S. W. Weng, T. Y. Lai and J. G. Chung, *Int. J. Oncol.*, 2010, **36**, 1113–1120.
7 M. L. Lin, J. G. Chung, Y. C. Lu, C. Y. Yang and S. S. Chen, *Oral Oncol.*, 2009, **45**, 531–537.
8 C. Y. Chang, H. L. Chan, H. Y. Lin, T. D. Way, M. C. Kao, M. Z. Song, Y. J. Lin and C. W. Lin, *J. Evidence-Based Complementary Altern. Med.*, 2012, **2012**, 952504.
9 J. F. Timms and R. Cramer, *Proteomics*, 2008, **8**, 4886–4897.
10 P. H. Hung, Y. W. Chen, K. C. Cheng, H. C. Chou, P. C. Lyu, Y. C. Lu, Y. R. Lee, C. T. Wu and H. L. Chan, *Mol. BioSyst.*, 2011, **7**, 1990–1998.
11 H. L. Huang, H. W. Hsing, T. C. Lai, Y. W. Chen, T. R. Lee, H. T. Chan, P. C. Lyu, C. L. Wu, Y. C. Lu, S. T. Lin, C. W. Lin, C. H. Lai, H. T. Chang, H. C. Chou and H. L. Chan, *J. Biomed. Sci.*, 2010, **17**, 36.
12 H. C. Chou, Y. W. Chen, T. R. Lee, F. S. Wu, H. T. Chan, P. C. Lyu, J. F. Timms and H. L. Chan, *Free Radicals Biol. Med.*, 2010, **49**, 96–108.
13 S. T. Lin, H. C. Chou, S. J. Chang, Y. W. Chen, P. C. Lyu, W. C. Wang, M. D. Chang and H. L. Chan, *J. Proteomics*, 2012, **75**, 5822–5847.
14 J. Y. Chen, H. C. Chou, Y. H. Chen and H. L. Chan, *J. Nutr. Biochem.*, 2013, **24**, 1889–1910.
15 H. L. Chan, S. Gharbi, P. R. Gaffney, R. Cramer, M. D. Waterfield and J. F. Timms, *Proteomics*, 2005, **5**, 2908–2926.
16 H. C. Chou, Y. C. Lu, C. S. Cheng, Y. W. Chen, P. C. Lyu, C. W. Lin, J. F. Timms and H. L. Chan, *J. Proteomics*, 2012, **75**, 3158–3176.
17 C. L. Wu, H. C. Chou, C. S. Cheng, J. M. Li, S. T. Lin, Y. W. Chen and H. L. Chan, *J. Proteomics*, 2012, **75**, 1991–2014.
18 Y. H. Chen, H. C. Chou, S. T. Lin, Y. W. Chen, Y. W. Lo and H. L. Chan, *J. Proteomics*, 2012, **77**, 111–128.
19 T. C. Lai, H. C. Chou, Y. W. Chen, T. R. Lee, H. T. Chan, H. H. Shen, W. T. Lee, S. T. Lin, Y. C. Lu, C. L. Wu and H. L. Chan, *J. Proteome Res.*, 2010, **9**, 1302–1322.
20 C. P. Lin, Y. W. Chen, W. H. Liu, H. C. Chou, Y. P. Chang, S. T. Lin, J. M. Li, S. F. Jian, Y. R. Lee and H. L. Chan, *Mol. BioSyst.*, 2012, **8**, 1136–1145.
21 Y. W. Chen, J. Y. Liu, S. T. Lin, J. M. Li, S. H. Huang, J. Y. Chen, J. Y. Wu, C. C. Kuo, C. L. Wu, Y. C. Lu, Y. H. Chen, C. Y. Fan, P. C. Huang, C. H. Law, P. C. Lyu, H. C. Chou and H. L. Chan, *Mol. BioSyst.*, 2011, **7**, 3065–3074.
22 C. Y. Chang, H. L. Chan, H. Y. Lin, T. D. Way, M. C. Kao, M. Z. Song, Y. J. Lin and C. W. Lin, *J. Evidence-Based Complementary Altern. Med.*, 2012, **2012**, 952504.
23 S. Lin, M. Fujii and D. X. Hou, *Arch. Biochem. Biophys.*, 2003, **418**, 99–107.
24 E. Buytaert, J. Y. Matroule, S. Durinck, P. Close, S. Kocanova, J. R. Vandenheede, P. A. de Witte, J. Piette and P. Agostinis, *Oncogene*, 2008, **27**, 1916–1929.
25 H. L. Chan, P. R. Gaffney, M. D. Waterfield, H. Anderle, M. H. Peter, H. P. Schwarz, P. L. Turecek and J. F. Timms, *FEBS Lett.*, 2006, **580**, 3229–3236.
26 J. L. Chen, J. Y. Wang, Y. F. Tsai, Y. H. Lin, L. M. Tseng, W. C. Chang, K. L. King, W. S. Chen, J. H. Chiu and Y. M. Shyr, *Menopause*, 2013, **20**, 646–654.
27 W. W. Lai, J. S. Yang, K. C. Lai, C. L. Kuo, C. K. Hsu, C. K. Wang, C. Y. Chang, J. J. Lin, N. Y. Tang, P. Y. Chen, W. W. Huang and J. G. Chung, *In Vivo*, 2009, **23**, 309–316.
28 M. L. Lin, J. G. Chung, Y. C. Lu, C. Y. Yang and S. S. Chen, *Oral Oncol.*, 2009, **45**, 531–537.
29 L. C. Chen, I. C. Chung, C. Hsueh, N. M. Tsang, L. M. Chi, Y. Liang, C. C. Chen, L. J. Wang and Y. S. Chang, *Cell Death Differ.*, 2010, **17**, 1463–1473.
30 Z. Y. Chen, L. Cai, J. Zhu, M. Chen, J. Chen, Z. H. Li, X. D. Liu, S. G. Wang, P. Bie, P. Jiang, J. H. Dong and X. W. Li, *Carcinogenesis*, 2011, **32**, 1419–1426.
31 Y. F. Feng, T. Li, S. Li, J. R. Peng and X. S. Leng, *Zhonghua Ganzangbing Zazhi*, 2009, **17**, 649–652.
32 T. Kobayashi, T. Shimura, T. Yajima, N. Kubo, K. Araki, W. Wada, S. Tsutsumi, H. Suzuki, H. Kuwano and A. Raz, *Clin. Exp. Metastasis*, 2011, **28**, 367–376.
33 T. Fukumori, Y. Takenaka, N. Oka, T. Yoshii, V. Hogan, H. Inohara, H. O. Kanayama, H. R. Kim and A. Raz, *Cancer Res.*, 2004, **64**, 3376–3379.
34 N. Oka, S. Nakahara, Y. Takenaka, T. Fukumori, V. Hogan, H. O. Kanayama, T. Yanagawa and A. Raz, *Cancer Res.*, 2005, **65**, 7546–7553.
35 C. Bonfils, N. Bec, C. Larroque, M. Del Rio, C. Gongora, M. Pugniere and P. Martineau, *Biochem. Biophys. Res. Commun.*, 2010, **393**, 325–330.
36 C. Wang and R. J. Youle, *Annu. Rev. Genet.*, 2009, **43**, 95–118.
37 A. Floridi, S. Castiglione and C. Bianchi, *Biochem. Pharmacol.*, 1989, **38**, 743–751.

38 Z. Q. Ji, C. W. Huang, C. J. Liang, W. W. Sun, B. Chen and P. R. Tang, *Zhonghua Kouqiang Yixue Zazhi*, 2005, **85**, 1836–1841.
39 N. N. Danial, L. D. Walensky, C. Y. Zhang, C. S. Choi, J. K. Fisher, A. J. Molina, S. R. Datta, K. L. Pitter, G. H. Bird, J. D. Wikstrom, J. T. Deeney, K. Robertson, J. Morash, A. Kulkarni, S. Neschen, S. Kim, M. E. Greenberg, B. E. Corkey, O. S. Shirihai, G. I. Shulman, B. B. Lowell and S. J. Korsmeyer, *Nat. Med.*, 2008, **14**, 144–153.
40 N. N. Danial, C. F. Gramm, L. Scorrano, C. Y. Zhang, S. Krauss, A. M. Ranger, S. R. Datta, M. E. Greenberg, L. J. Licklider, B. B. Lowell, S. P. Gygi and S. J. Korsmeyer, *Nature*, 2003, **424**, 952–956.
41 D. Shenton and C. M. Grant, *Biochem. J.*, 2003, **374**, 513–519.
42 M. E. Weeks, J. Sinclair, A. Butt, Y. L. Chung, J. L. Worthington, C. R. Wilkinson, J. Griffiths, N. Jones, M. D. Waterfield and J. F. Timms, *Proteomics*, 2006, **6**, 2772–2796.
43 M. Kemp, Y. M. Go and D. P. Jones, *Free Radicals Biol. Med.*, 2008, **44**, 921–937.
44 J. V. Cross and D. J. Templeton, *Antioxid. Redox Signaling*, 2006, **8**, 1819–1827.
45 L. K. Moran, J. M. Gutteridge and G. J. Quinlan, *Curr. Med. Chem.*, 2001, **8**, 763–772.
46 P. Ghezzi, V. Bonetto and M. Fratelli, *Antioxid. Redox Signaling*, 2005, **7**, 964–972.

